

01 Sep 2011

Coaxial Cable Bragg Grating

Tao Wei

Songping Wu

Jie Huang

Missouri University of Science and Technology, jieh@mst.edu

Hai Xiao

Missouri University of Science and Technology, xiaoha@mst.edu

et. al. For a complete list of authors, see https://scholarsmine.mst.edu/ele_comeng_facwork/3258

Follow this and additional works at: https://scholarsmine.mst.edu/ele_comeng_facwork



Part of the [Electrical and Computer Engineering Commons](#)

Recommended Citation

T. Wei et al., "Coaxial Cable Bragg Grating," *Applied Physics Letters*, vol. 99, no. 11, American Institute of Physics (AIP), Sep 2011.

The definitive version is available at <https://doi.org/10.1063/1.3636406>

This Article - Journal is brought to you for free and open access by Scholars' Mine. It has been accepted for inclusion in Electrical and Computer Engineering Faculty Research & Creative Works by an authorized administrator of Scholars' Mine. This work is protected by U. S. Copyright Law. Unauthorized use including reproduction for redistribution requires the permission of the copyright holder. For more information, please contact scholarsmine@mst.edu.

Coaxial cable Bragg grating

Tao Wei, Songping Wu, Jie Huang, Hai Xiao,^{a)} and Jun Fan^{a)}

Department of Electrical and Computer Engineering, Missouri University of Science and Technology, Rolla, Missouri 65409, USA

(Received 18 May 2011; accepted 12 August 2011; published online 16 September 2011)

This paper reports a coaxial cable Bragg grating (CCBG) fabricated by drilling holes into the cable at periodic distances along the axial direction. Resonances were observed at discrete frequencies in both transmission and reflection spectra. The analogy of the CCBG with a fiber Bragg grating is shown. The grating was tested for the potential application as a strain-sensing device. © 2011 American Institute of Physics. [doi:10.1063/1.3636406]

Coaxial cable and optical fiber are the two types of cylindrical waveguiding media used in telecommunications for transmitting signals over a long distance. Governed by the same electromagnetic (EM) theory, the two share the common fundamental physics to confine and guide EM waves. However, the frequencies of the EM waves supported by them are quite different. The optical frequency is orders of magnitude higher than the radio frequency (RF). Over the years, optical fiber and coaxial cable technologies have evolved along quite different paths, resulting in unique devices of their own. An interesting question is that some of the established concepts of fiber optic devices can be adopted onto the coaxial cable. This is not only interesting from the device physics perspective but also motivated by the application potentials that the coaxial cable device might provide a solution for some challenging issues faced by fiber optic devices, especially when the device is used as a sensor.

Pioneering research has already started to explore various coaxial cable devices mimicking their optical fiber counterparts. Inspired by the well-known optical fiber Mach-Zehnder interferometer (MZI), Sánchez-López *et al.* implemented a linear passive MZI using coaxial cables and demonstrated superluminal and negative group velocity in the RF regime.¹ Dorion *et al.* used a sequence of electronic phase shifters and partial reflectors/transmitters to form a 1 kHz electronic laser.² RF bandgap structures have also been explored to mimic the photonic crystal (PC) devices that have found many interesting applications in optics such as wavelength specific filters, reflectors, waveguides, light trappers, and superlenses.³ In one case, alternating 50 Ω and 93 Ω coaxial cable segments were connected in a row to create periodic impedance variations along the cable length to form the so called coaxial PC.⁴ Experimental evidence such as bandgap, sub- or superluminal velocities, and defect modes were observed and investigated in the electric range.⁵⁻⁷

Unlike the strong-contrasted alternating multiple dielectric layers or lattices in a typical PC structure, fiber Bragg grating (FBG) weakly modifies its refractive index along the optical fiber axial direction, resulting in strong, narrow-band reflections at discrete resonant wavelengths. FBGs have found many applications in optical communications, for

example, as an add-drop filter, multiplexer, or dispersion compensator.⁸ Also, FBGs are extensively used as sensors for measurements of various parameters such as strain, temperature, pressure, and vibration.⁹ Recently, there is an increasing interest in using FBGs in structural health monitoring (SHM) because FBGs can be embedded in a structure and multiplexed to measure strain distribution with high sensitivity.¹⁰ However, optical fibers are fragile and can easily break when they are subject to a strain larger than about 4000 $\mu\epsilon$ making it difficult to install and operate the sensors for SHM in harsh environment.

On the other hand, coaxial cables are large in diameter and can survive a large strain. If the Bragg grating concept can be implemented on a coaxial cable, the resulted coaxial cable Bragg grating (CCBG) sensor may provide a viable solution for large strain measurement which is long desired in SHM. In this work, we report the implementation of the Bragg grating concept using a coaxial cable, understanding of device physics, and demonstration of such a CCBG for strain measurement.

Shown in Fig. 1(a), the CCBG is fabricated by drilling open holes at periodic distance along a coaxial cable using a drilling machine. In our experiments, a SubMiniature version A connector (SMA) type coaxial cable (RG-58/U) made by Jameco Electronics was used. The cable has a solid bare copper inner conductor with a diameter of 0.812 mm, a dielectric layer made of solid polyethylene with a diameter of 2.95 mm, an outer conductor made of tinned copper braid, and a plastic cable jacket with a diameter of 4.95 mm. Prior hole-drilling, a small section of the cable jacket was cut off to expose the outer conductor. The hole-drilling was carried out by using a 1/8 in. drill bit and then enlarged by an 11/64 in. bit. For each hole, the drilling process stopped immediately as the drilling bit tip approached the inner conductor. The pitch, Λ (i.e., the period of the grating) defined as the

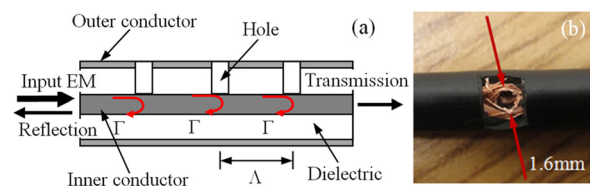


FIG. 1. (Color online) Coaxial cable Bragg gratings. (a) Schematics, (b) microscopic image of drilled open hole.

^{a)}Authors to whom correspondence should be addressed. Electronic addresses: xiaoha@mst.edu and jfan@mst.edu.

distance in between two neighboring holes, was 6.4 cm. A total of 23 holes (i.e., 22 periods) were drilled along the cable. Fig. 1(b) shows the microscopic image of a single drilled hole on the coaxial cable. The diameter of the hole is approximately 1.6 mm measured by a caliper. The depth of hole was measured to be about 1 mm using a measuring microscope by focusing onto the valley of the hole and the top of the cylindrical surface.

A vector network analyzer (VNA, Agilent E5071C) was used to acquire the transmission and reflection spectra of the CCBG by measuring the insertion loss (S_{21}) and the return loss (S_{11}) in the frequency range from 100 kHz to 8 GHz with a total number of scanning points 1601. Fig. 2(a) and 2(b) plot the transmission and reflection spectra of the CCBG, respectively. The spectra of the coaxial cable before hole-drilling were also plotted in Fig. 2 for comparison. It is quite clear that resonance bands at discrete frequencies have shown in both the transmission and admission spectra of the cable after periodic holes have been drilled. The fundamental frequency of this specific device was at 1.56 GHz. High frequency resonances occurred at the integer numbers of the fundamental frequency. In the transmission spectra, a background frequency-dependent loss can be seen. The higher the frequency is, the larger the loss becomes. However, the background loss line of the CCBG device matched well with the original cable, indicating that the hole-drilling did not incur in any observable extra loss to the cable. Similar resonance behavior has also been observed on the reflection spectrum. The resonances shown in the transmission spectrum matched exactly those in the reflection spectra. It is also worth noting that in the reflection spectra, the noise level is contributed by multiple reflections due to the imperfection of the cable and the connectors.

An analytical model based on wave propagation theory was employed to understand the physics of CCBG. By drilling a hole into a coaxial cable, one perturbs the EM waves in the otherwise continuous coaxial transmission line, resulting in a localized characteristic impedance change and thus a partial reflection from the impedance discontinuity. Assuming that all the discontinuities are identical, each hole generates a partial reflection with a reflection coefficient Γ as shown in Fig. 1(a). Further assuming that the initial phase at the first hole is zero and the cable is lossless as the voltage

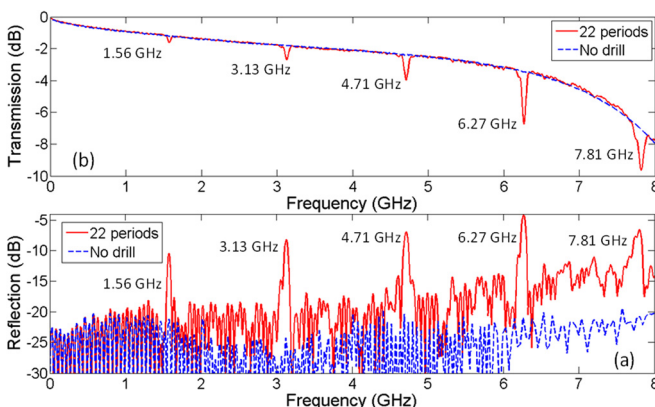


FIG. 2. (Color online) Reflection and transmission spectra of a coaxial cable with and without drilled holes.

wave travels along the coaxial cable, the accumulated reflection (S_{11}) can be derived by the following equation:¹¹

$$S_{11} = \frac{1}{V_0} \sum_{n=0}^{N-1} V_r[n] e^{-j2\beta n\Lambda}, \quad (1)$$

where V_0 is the input voltage wave, N is the total number of holes on the cable, $V_r[n]$ is the reflected voltage wave at the n_{th} hole, β is the propagation constant of the EM wave traveling inside the coaxial cable, Λ is the period of grating, and $2\beta n\Lambda$ is the phase difference of a wave traveling a round-trip between the first and the n_{th} hole. The propagation constant β can be calculated by $\beta = 2\pi f \sqrt{LC}$, where f is the frequency of the EM wave and L and C are the distributed (per unit length) inductance and capacitance of the cable, respectively.

Assuming a small reflection coefficient of each hole, waves that reflected more than once carry very little energy so that multiple reflections can be neglected. Given that the transmission coefficient of a hole is $(1 + \Gamma)$, $V_r[n]$, can be written as $V_0 \Gamma (1 + \Gamma)^{2n}$.¹¹ Therefore, the accumulated reflection given in Eq. (1) can be simplified as

$$S_{11} = \frac{\Gamma [1 - (1 + \Gamma)^{2N} e^{-2j\beta N\Lambda}]}{1 - (1 + \Gamma)^2 e^{-2j\beta\Lambda}}. \quad (2)$$

A commercial software package (Ansoft HFSS) was used to calculate the reflection coefficient in Eq. (2). The finite element method can analyze the open-hole structure induced EM perturbation. Using the cable parameters from its datasheet and the measured dimensions of the hole, we calculated the magnitude of the reflection coefficient of a single hole. As shown in the inset of Fig. 3, the simulation results indicate that the reflection coefficient increases linearly as a function of frequency. Once the reflection coefficient is determined, the reflection spectrum of the CCBG can be calculated using Eq. (2). The propagation constant β was calculated using the cable parameters from datasheet, where $C = 100$ pF/m and $Z = \sqrt{L/C} = 50 \Omega$. As such, the distributed inductance is 250 nH/m.

Fig. 3 plots the simulated reflection spectra (S_{11}) of two CCBGs with the same period (6.4 cm) and open-hole geometry but different grating lengths (7 and 23 holes). Within the observation bandwidth of 100 kHz-8 GHz, discrete resonances can be seen at the fundamental frequency of 1.575 GHz and its harmonics. The resonance bands of the two CCBGs happened at the same location but the longer grating had stronger resonances with a higher Q-factor. In the simulated

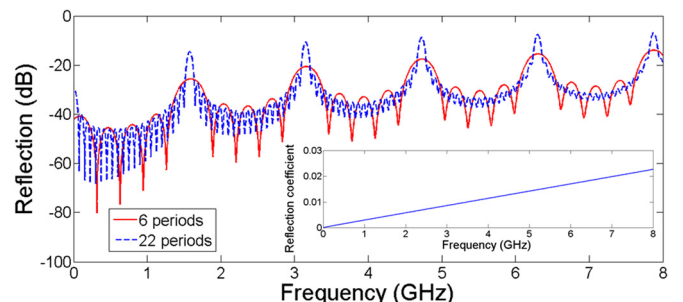


FIG. 3. (Color online) Simulated reflection spectra with 6 and 22 periods. Inset: reflection coefficient of a single open hole as a function of frequency.

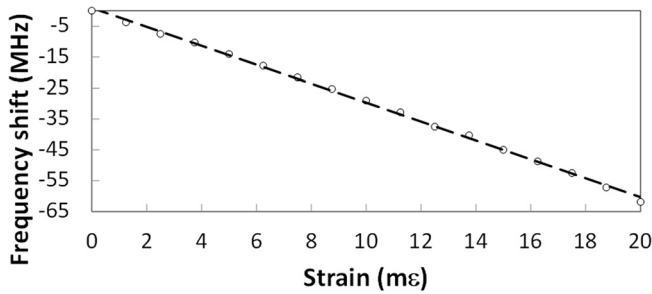


FIG. 4. Resonant frequency as a function of strain.

reflection spectrum, the resonant peak strength increased as frequency increased. This can be qualitatively explained by the increasing reflection coefficient as a function of frequency shown in the inset. In the measured reflection spectra (Fig. 2), the resonant peak has an increasing strength (up to the fourth harmonic) as frequency increased and then a slightly decreased strength in the fifth harmonic. We believe this is because a lossless cable was assumed in the model while the cable used in the experiments had a higher loss at higher frequency as indicated in Fig. 2(a). Examining Eq. (1), one realizes that the reflection spectrum S_{11} is in the form of the discrete Fourier transform of the reflected voltage wave $V_r[n]$. Given that the reflection coefficient is small, $V_r[n]$ is approximately the same, resulting in a Sinc function in the frequency domain. This explains the existence of the side lobes around each resonant peak.

Similar to the well-studied case of fiber Bragg gratings, where the forward propagating mode is coupled to backward propagating mode in the waveguide at discrete resonant frequencies satisfying the following Bragg condition:⁹

$$\beta^+ - \beta^- = 2\beta = \frac{2m\pi}{\Lambda} \quad \text{or} \quad f_{res}^m = \frac{m}{2\Lambda\sqrt{LC}}, \quad (3)$$

where β^+ and β^- are the propagation constants of the forward and backward traveling waves, respectively. They have the same magnitude but opposite signs. The resonant frequency is represented as f_{res} , and m is an integer representing the diffraction order of the grating. A quick calculation based on Eq. (3) revealed that the fundamental resonant frequency of the CCBG was 1.575 GHz given that the period was 6.4 cm. Comparing Figs. 2(b) and 3, in general the experimental and simulation results matched in terms of resonant frequency and quality factor. In Fig. 2(b), the side lobes of the Sinc function are not clearly identifiable as in Fig. 3. This may be because of the background noise caused by connector mismatch and non-equal distance between the holes.

Strain measurement was conducted to demonstrate the capability of using CCBG as a sensing device. The CCBG used for strain measurement had a pitch length of 2.5 cm and 45 periods, generating a series of resonances with the fundamental frequency of 4.25 GHz. The CCBG was mounted on a load frame (MTS 880 by TestResources Inc.) using two home machined aluminum clampers and interrogated by a VNA (HP 8753ES). The VNA was configured to acquire the first fundamental resonant peak in the reflection spectrum with an observation bandwidth from 3.5 to 5 GHz and a total of 1601 sampling points.

The reflection spectra of the CCBG with and without the clamping fixtures had no evident difference, indicating that the clampers did not introduce noticeable impedance mismatch and reflections. The load frame elongated the CCBG at a step of 0.05 in., corresponding to a strain increase of about 1.25 mε, given the initial distance between the two clampers is 40 in. Sixteen loading steps or a total strain of about 20 mε were applied to the CCBG using the load frame. For each strain point the reflection spectrum was measured multiple times consecutively, and the averaged spectrum was used to find the center frequency of the fundamental resonant peak. Fourth-order polynomial curve-fitting was used to smooth the resonant peak for further improvement of the measurement accuracy.

Fig. 4 plots the change in resonant frequency of the fundamental peak as a function of the applied strain. In general, the CCBG resonant frequency decreased almost linearly with a slope of about -3 kHz/ $\mu\epsilon$ as the applied strain increased. This is understandable because the stretch of the CCBG increased the period of the grating, resulting in a linear decrease of the resonant frequency as predicted by Eq. (3). The linear strain-frequency shift relation indicates that CCBG can be used as a sensor for strain measurement after it is properly calibrated. The CCBG survived 20 mε without cable-breakage, indicating a large strain capability of the CCBG in comparison with a FBG which typically survives a strain up to about 4 mε. The unique large strain capability and robustness to survive harsh conditions may enable applications in structural health monitoring.

To summarize, this paper reports a coaxial cable Bragg grating fabricated by drilling holes into the cable at periodic distances along the cable axis. The periodic impedance discontinuities produced resonant peaks in both transmission and reflection spectra at discrete frequencies. The theoretically simulated and experimentally measured resonant frequencies matched well. The resonant frequency of the CCBG device showed a linear response to the loaded strain. It is anticipated that there are many potential methods to create the impedance discontinuities in a coaxial cable besides that hole-drilling method. Also, the CCBG concept could lead to many potential sensing applications.

This work is supported by the National Science Foundation under Grant No. CMMI-1100185.

¹M. M. Sánchez-López, A. Sánchez-Meroño, J. Arias, J. A. Davis, and I. Moreno, *Appl. Phys. Lett.* **93**(7), 074102 (2008).

²S. Doiron, C. Giller, N. Beaudoin, and A. Haché, *Am. J. Phys.* **76**(11), 996 (2008).

³J. D. Joannopoulos, P. R. Villeneuve, and S. Fan, *Nature* **386**(6621), 143 (1997).

⁴J. N. Munday and W. M. Robertson, *Appl. Phys. Lett.* **83**(5), 1053 (2003).

⁵M. D. M. Sánchez-López, J. A. Davis, and K. Crabtree, *Am. J. Phys.* **71**(12), 1314 (2003).

⁶A. Haché and A. Slimani, *Am. J. Phys.* **72**(7), 916 (2004).

⁷G. J. Schneider, S. Hanna, J. L. Davis, and G. H. Watson, *J. Appl. Phys.* **90**(6), 2642 (2001).

⁸K. O. Hill and G. Meltz, *J. Lightwave Technol.* **15**(8), 1263 (1997).

⁹A. D. Kersey, M. A. Davis, H. J. Patrick, M. LeBlanc, K. P. Koo, C. G. Askins, M. A. Putnam, and E. J. Friebele, *J. Lightwave Technol.* **15**(8), 1442 (1997).

¹⁰M. Majumder, T. K. Gangopadhyay, A. K. Chakraborty, K. Dasgupta, and D. K. Bhattacharya, *Sens. Actuators A: Phys.* **147**(1), 150 (2008).

¹¹D. M. Pozar, *Microwave Engineering* (John Wiley & Sons, Hoboken, NJ, 2005), p. 52.